Bull. Natl. Mus. Nat. Sci., Ser. C, 48, pp. 1–14, December 23, 2022

DOI: 10.50826/bnmnsgeopaleo.48.0_1

Zircon U–Pb dating of Cretaceous Nishisonogi granites, western Nagasaki Prefecture, Kyushu, southwest Japan

Yukiyasu Tsutsumi[1, 2, *] **and Kenichiro Tani**[1]

[1]Department of Geology and Paleontology, National Museum of Nature and Science
4–1–1 Amakubo, Tsukuba, Ibaraki 305–0005, Japan
[2]Faculty of Life and Environmental Sciences, University of Tsukuba,
1–1–1 Tennodai, Tsukuba, Ibaraki 305–8572, Japan
*Author for correspondence: ytsutsu@kahaku.go.jp

Abstract The Nishisonogi granites are exposed at the northwestern end of the Nishisonogi Peninsula and some small islands up to the Goto Islands. In this study, Zircon U–Pb ages of 6 samples are measured and 4 effective ages are obtained from the granitic unit. Samples from Otateshima Island, Irose Islet, Enoshima Island and Hirukojima Island indicate ages of 97.1 ± 1.1 Ma, 99.5 ± 1.1 Ma, 100.5 ± 1.0 Ma and 102.0 ± 1.2 Ma, respectively, while the sample from Kotatejima Island indicates no effective age likely because its zircon grains are inherited. Although no effective age of the sample from Oseto located at the northwestern end of the Nishisonogi Peninsula was obtained, the formation age of the sample is thought to be ca. 95 Ma according to the mode of the probability density curve. Therefore, formation ages of the Nishisonogi granite range from 102 to 95 Ma, and the ages become older toward the continental side. This is opposite to the age tendency of granite in the Ryoke and Sanyo belts to be younger toward the continental side. This difference suggests it remains premature to identify the Nishisonogi granites as a western extension of the Ryoke and Sanyo belts.

Key words: plutonic age, granitoid, Nagasaki, Ainoshima zone, Ryoke

Introduction

While the geology of southwest Japan generally features zonal structures, they become disturbed in Kyushu, the western end of southwest Japan. Kyushu is tectonically subdivided to three parts, northern, central and southern Kyushu, by the Matsuyama-Imari tectonic line (TL) and Usuki-Yatsushiro TL. There have been a lot of opinions published about the geological framework of central Kyushu since the beginning of the 20th century. One of the earliest was by von Richthofen (1903), who coined the name “das Nagasaki Dreiecke (the Nagasaki triangular area).” Because the area has features of both the inner and outer zones of southwest Japan, the Nagasaki triangular area was thought to be the boundary between them.

High -P/T type metamorphics called the Nagasaki metamorphic rocks (Karakida *et al.*, 1969) outcrop at the western end of the area. After active discussion on the attribution of these metamorphics, Nishimura (1998) showed that they are composed of two different metamorphics: one showing relatively high metamorphic grades with Late Cretaceous white mica K–Ar ages, and another showing relatively low metamorphic grades with Permo-Jurassic white mica K–Ar ages. These two types of metamorphics are considered to be attributed to the Sanbagawa and Suo belts, respectively. In this sense, the Nagasaki metamorphic rocks combine the features of both inner and outer zones of southwest Japan. Currently, only the younger metamorphics are referred to as the Nagasaki Metamorphic Complex (NMC), and older metamorphics are thought to belong to a western extension of the Suo Metamorphic Belt (SMB; e.g. Miyazaki *et al.*, 2013). The tectonic boundary between the NMC and SMB is recognized in two areas in the Nagasaki Peninsula, the Fukahori–Wakimisaki Thrust and the Mogi Thrust at the western and eastern parts of the peninsula, respectively (Nishimura *et al.*, 2004). The NMC appears as a window in the SMB in the peninsula. On the other hand, all metamorphics in the Nishisonogi Peninsula are attributed to the NMC. Differences in protolith and deposition ages between NMC and SMB are confirmed by the age

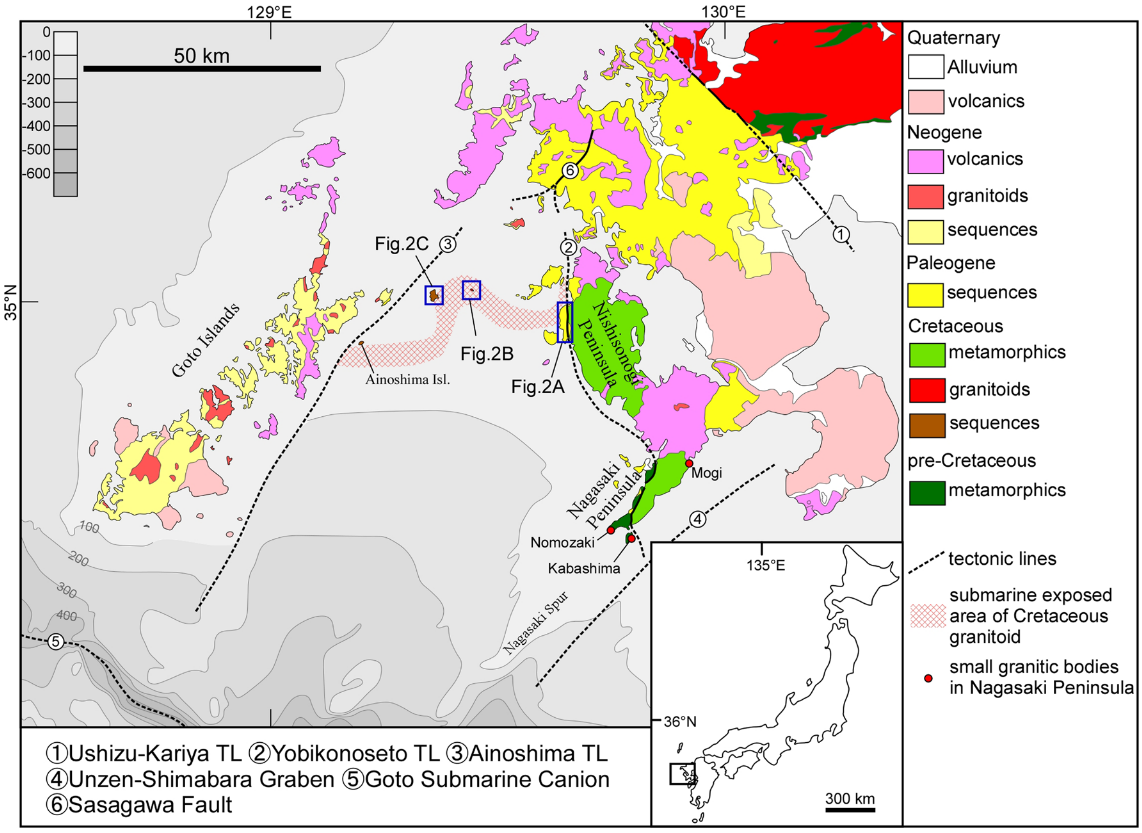

Fig. 1. Geological map of northwestern Kyusyu. Submarine exposed area of Cretaceous granitoids is from Tachibana (1962).

spectrum of detrital zircons (Kochi *et al.*, 2011; Tsutsumi *et al.*, 2003). Submarine geography and geologic structure in western Kyushu are complicated because of influence from the opening of the Sea of Japan in the Oligocene through to Miocene as well as the Okinawa Trough, which has continued since the Late Miocene. It is divided into several zones, including the Nishisonogi, Ainoshima, Goto and Tsushima zones (Isomi *et al.*, 1971). The Ainoshima zone (or block) is bounded by the Yobikonoseto TL, Ainoshima TL, Goto Submarine Canyon and extension of the Unzen-Shimabara Graben (e.g. Katsura, 1992). Because it is assumed that the Fukahori–Wakimisaki Thrust continues to the Yobikonoseto TL (Nishimura *et al.*, 2004), the SMB on the western side of the Nagasaki Peninsula is thought to be attributed to this zone.

Cretaceous granitoids in the Nagasaki Prefecture are scarce and all of them outcrop as small intrusions or tectonic blocks that are not recognizable in large scale maps such as Fig. 1. In the Nagasaki Peninsula, Cretaceous granitoid intrusions in the SMB are recognized in Nomozaki and Kabashima (Fig. 1). The zircon U–Pb age of the granitoid in Kabashima is 118.0 ± 0.8 Ma (95% conf., Nagata *et al.*, 2020) whereas biotite and muscovite K–Ar ages of the granitoid are 93.0–77.1 Ma (Hattori and Shibata, 1982; Nishimura, 1998). Granitic tectonic blocks are recognized in the Mogi area (Nishimura *et al.*, 2004). The zircon U–Pb age of one of these blocks was determined to be 117.1 ± 0.4 Ma (95% conf., Tsutsumi and Horie, 2019). Based on these zircon age data, the formation ages of granitoids in the Nagasaki Peninsula are thought to be 118–117 Ma, Early Cretaceous in age. On the other hand, the Nishisonogi granites (Tachibana, 1962) are exposed in the northwestern part of the Nishisonogi Peninsula and several islands in the northern part of the Ainoshima zone and have biotite K–Ar ages of 93.1–89.2 Ma (Hattori and Shibata, 1982). It is thought that Nishisonogi granites occur not only in islands but also in the seafloor in the northern part of the Ainoshima zone (Tachibana, 1962). Moreover, high -P/T type metamorphics (unknown whether SBM or NMC) exist in the submarine Nagasaki Spur (Kimura *et al.*, 1975), and Cretaceous sequences exist in Enoshima and Ainoshima islands (Katada *et al.*, 1972). These observations

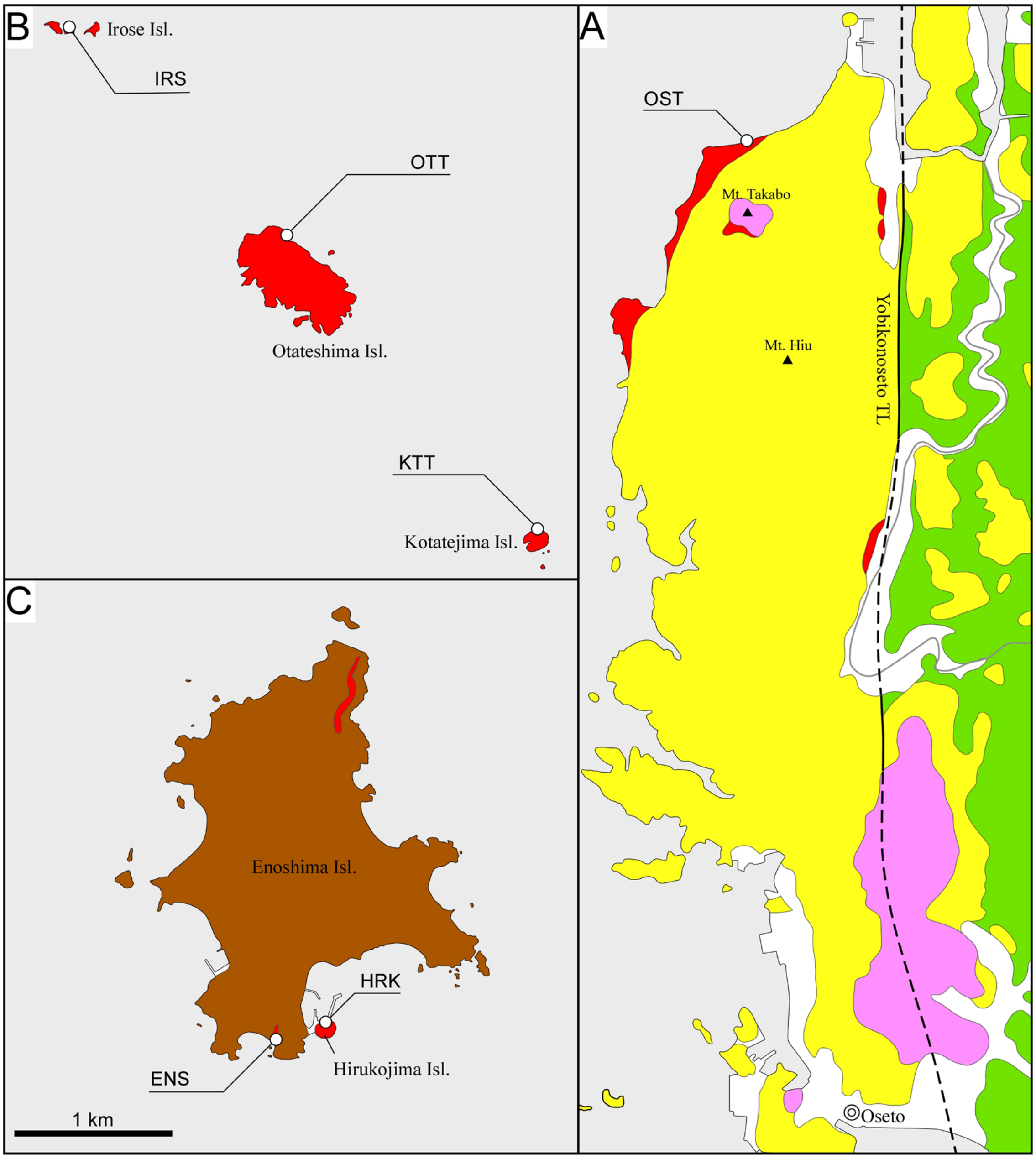

Fig. 2. Geological map around the sampling localities, modified after Hattori *et al.* (1993) and Katada *et al.* (1972). Legends are provided in Fig. 1.

show that pre-Paleogene rocks widely exist in all over the Ainoshima zone.

The Nishisonogi granites are thought to be a western extension of the Ryoke and Sanyo belts on the basis of their similar rock features (Tachibana, 1962) and radiometric ages (Hattori and Shibata, 1982). Moreover, the Oseto granodiorite in the northwestern end of the Nishisonogi Peninsula is thought to contact the NMC along the Yobikonoseto TL. This relationship is similar to the one between the Ryoke and Sanbagawa belts along the Median Tectonic Line (MTL). Because the Nishisonogi granites occur at the western end of southwest Japan, clarifying their ages is important to understand the western extension of the Ryoke and Sanyo belts.

Geological Setting

The Nishisonogi granites occur only in Oseto, the northwestern end of the Nishisonogi Peninsula and some islets north of Oseto, as well as the following small islands between the peninsula and Goto Islands: Kotatejima Island, Otateshima Island, Irose Islet, Enoshima Island and Hirukojima Island (Fig. 2).

Granitoids in Oseto are called Oseto granodiorites (Fig. 3A), which are sometimes found as lenticular deformed mafic magmatic enclaves (MMEs) (Fig. 3B). Biotite K–Ar age is 90 Ma (recalculated; Kawano and Ueda, 1966). Although a zircon U–Pb age of 99.8 ± 4.5 Ma (95% conf., MSWD = 9.6) was once reported for the Oseto granodiorites, very high dispersion of the data prohibiting calculation of an effectual weighted mean age suggests the possibility that xenocrysts were mixed in the analyzed zircon grains (Kochi *et al.*, 2011). The Oseto granodiorites are overlain by a Paleogene sequence of sedimentary rocks, of which the basal conglomerate layer includes granodiorites and pelitic schist pebbles that are thought to have been derived from the Oseto granodiorites and NMC, respectively (Fig. 3C). Rocks in small outcrops in Terashima Island, Kabutose Islet, as well as those close to Yobikonoseto TL, are highly fractured and altered.

Kotatejima Island (Fig. 3D, E), Otateshima Island (Fig. 3F, G) and Irose Islet (Fig. 3H, I) are composed of granitoids. Several pegmatite veins exist in these islands. Only a small amount of MMEs are present within the studied granitoid bodies. Biotite K-Ar ages of Kotatejima Island and Irose Islet were 93.1 ± 3.2 Ma and 92.6 ± 3.2 Ma, respectively (Hattori and Shibata, 1982).

Enoshima Island is composed mostly of the Cretaceous sequence consisting mainly of volcanics and volcaniclastics, and correlated to the Kanmon Group (Katada *et al.*, 1972). NNE–SSW trending granitic intrusion exists on the southern coast (Fig. 3J) and northern part. Hirukojima Island which is a small island adjacent to Enoshima Island, is composed mainly of granodiorite intrusions (Fig. 3K). Biotite K–Ar ages of the granodiorites are 92.4 ± 4.7 Ma and 89.2 ± 2.9 Ma (Hattori and Shibata, 1982).

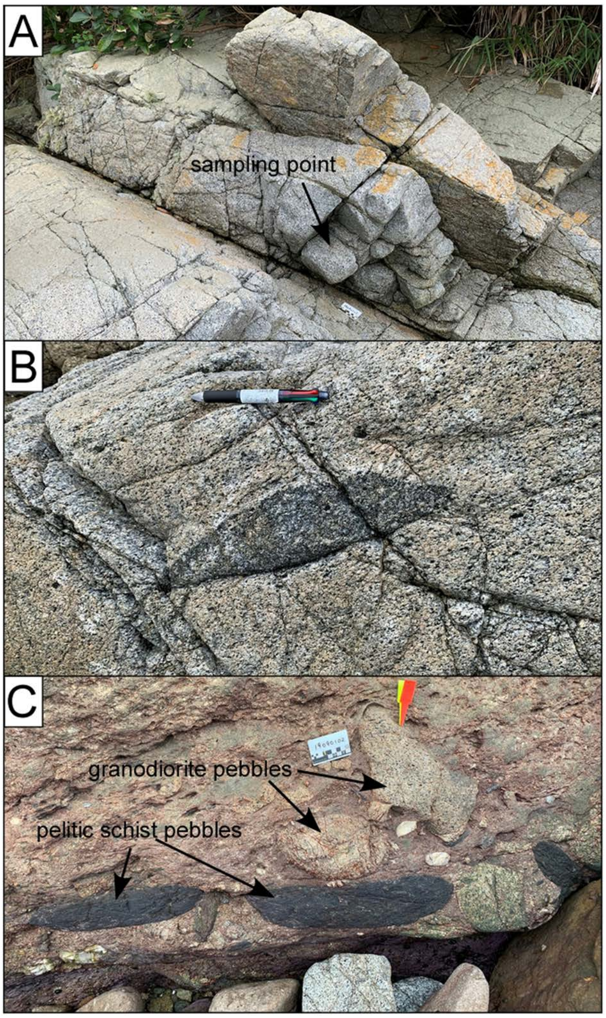

Fig. 3. Photographs of typical outcrops; A: An outcrop of the Oseto granodiorite (sample locality of OST). B: Lenticular MME in the Oseto granodiorite. C: Basal conglomerate of the Paleogene sedimentary sequence overlying the Oseto granodiorite. D and E: A view of Kotatejima Island and the sampling point of KTT, respectively. F and G: A view of Otateshima Island and the sampling point of OTT, respectively. H and I: A view of Irose Islet and the sampling point of IRS, respectively. J: The sampling point of ENS. K: the sampling point of HRK.

Analytical Methods

At first, the rock samples were scrubbed, and washed in an ultrasonic bath for ten minutes to avoid surface zircon contaminants. Fragmentation of the rock sample was conducted by a high voltage pulse power selective fragmentation equipment, SELFRAG Lab (Selfrag AG). The zircon grains were handpicked from heavy fractions that were separated through heavy-liquid techniques. Zircon grains from the samples, the zircon standards TEMORA2 (416.78 Ma; Black *et al.*, 2004) and OD-3 (33 Ma; Iwano *et al.*, 2013), and the glass standard NIST SRM610 were mounted in an epoxy resin and polished till the surface was flattened with the center of the embedded grains exposed. After the mounting and polishing, backscattered electron (BE) and cathodoluminescence (CL) images of zircon grains were taken. Scanning electron microscope-cathodoluminescence equipment, JSM-6610 (JEOL) and a CL detector (SANYU electron), were used for BE and CL images. The images were used

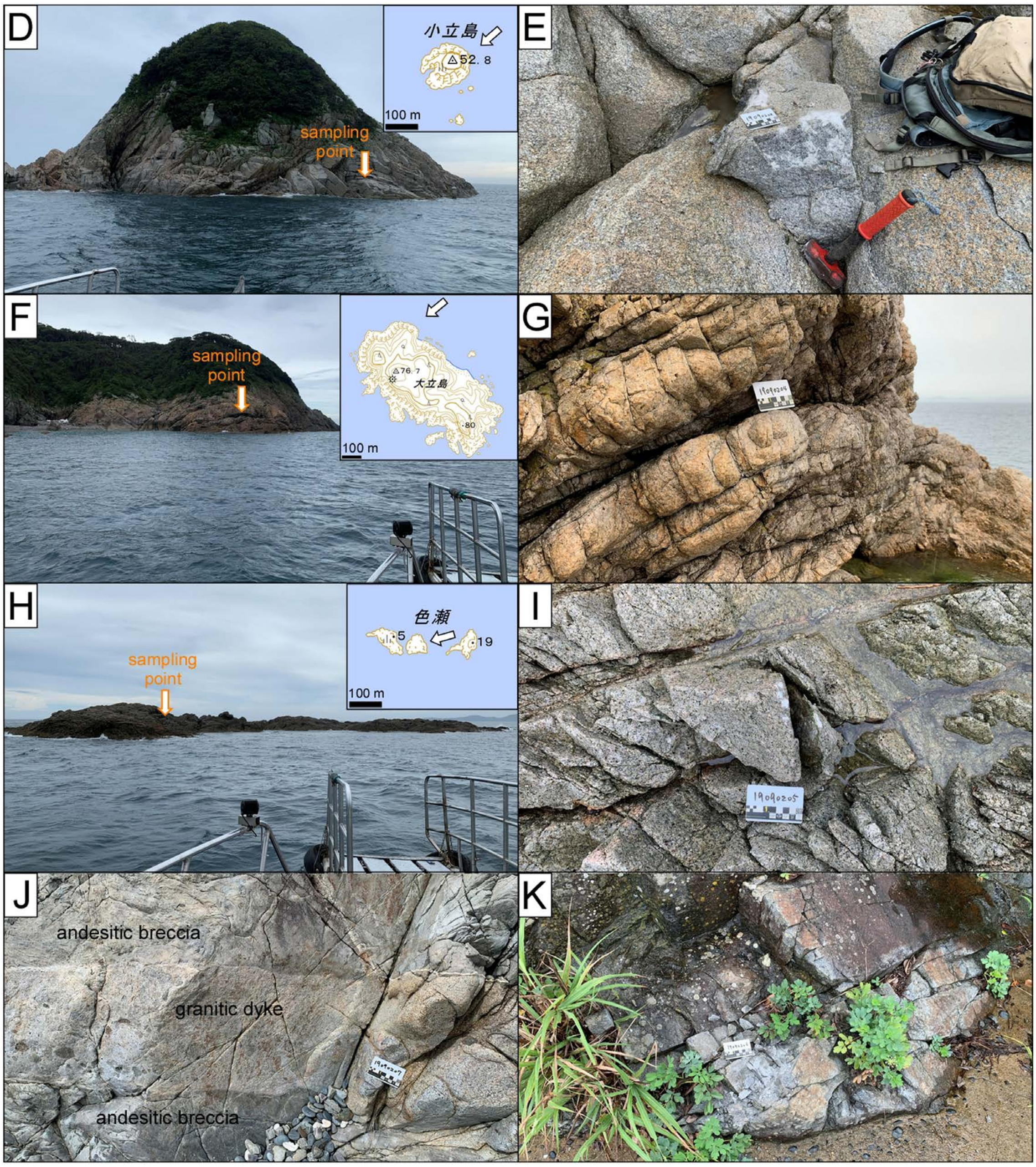

Fig. 3 (continued)

to select the sites for analysis. U–Pb dating of the samples was carried out using laser ablation inductively coupled plasma mass spectrometry using an NWR213 (Elemental Scientific Lasers) and Agilent 7700x (Agilent Technologies). All processes for sample preparation and analysis were conducted at the National Museum of Nature and Science, Tsukuba, Japan. The experimental conditions and the analytical procedures used for measurements followed Tsutsumi *et al.* (2012), with the additional devices of a buffered type stabilizer (Tunheng and Hirata, 2004) and TwoVol2 sample cell also applied. The spot size of the laser was 25 µm. A correction for common Pb was made on the basis of the measured ^{207}Pb/^{206}Pb ratio (^{207}Pb correction), ^{208}Pb/^{206}Pb and Th/U ratios (^{208}Pb correction) (e.g. Williams, 1998) and the model for common Pb compositions proposed by Stacey and Kramers (1975). In this paper, we adopt ^{207}Pb correction for age discussion because it is more effective for calculating Phanerozoic ^{238}U–^{206}Pb* age than ^{208}Pb correction (e.g. Williams, 1998). ^{208}Pb corrected ^{238}U/^{206}Pb* and ^{207}Pb*/^{206}Pb* ratios were used for concordia plots. Pb* indicates radiometric Pb. The pooled ages presented in this study were calculated using the IsoplotR software (Vermeesch, 2018). The data of secondary standard OD-3 zircon obtained during analysis yielded weighted mean ages of 33.6 ±

Table 1. LA-ICP-MS U–Pb data and calculated ages of zircons in the samples.

Labels	$^{206}Pb_c$ [(1)] (%)	U (ppm)	Th (ppm)	Th/U	$^{238}U/^{206}Pb^{*(1)}$	$^{207}Pb^*/^{206}Pb^{*(1)}$	$^{238}U–^{206}Pb^*$ age[(1)] (Ma)	$^{238}U–^{206}Pb^*$ age[(2)] (Ma)	Remarks
Oseto granodiorite (OST)									
OST_01.1	1.58	210	80	0.39	62.05 ± 1.24	0.0414 ± 0.0059	103.1 ± 2.0	103.9 ± 2.0	
OST_02.1	0.95	484	252	0.53	62.34 ± 1.16	0.0449 ± 0.0051	102.6 ± 1.9	103.0 ± 1.9	
OST_03.1	0.78	213	155	0.75	64.52 ± 1.14	0.0414 ± 0.0065	99.1 ± 1.7	99.9 ± 1.6	
OST_04.1	0.08	236	145	0.63	67.26 ± 1.37	0.0499 ± 0.0064	95.1 ± 1.9	94.9 ± 1.9	
OST_05.1	0.00	268	173	0.66	65.42 ± 1.09	0.0469 ± 0.0029	97.8 ± 1.6	97.8 ± 1.6	
OST_06.1	1.88	199	113	0.58	67.97 ± 1.44	0.0551 ± 0.0084	94.2 ± 2.0	93.3 ± 1.9	
OST_07.1	0.00	289	207	0.74	66.70 ± 1.11	0.0500 ± 0.0032	95.9 ± 1.6	95.7 ± 1.6	
OST_08.1	0.37	165	116	0.72	62.80 ± 1.30	0.0474 ± 0.0071	101.8 ± 2.1	101.9 ± 2.0	
OST_09.1	0.60	137	139	1.04	64.29 ± 1.56	0.0414 ± 0.0098	99.5 ± 2.4	100.1 ± 2.2	
OST_09.2	0.38	142	61	0.44	65.54 ± 1.33	0.0430 ± 0.0057	97.6 ± 2.0	98.0 ± 1.9	
OST_10.1	0.00	483	419	0.89	64.80 ± 1.00	0.0448 ± 0.0019	98.7 ± 1.5	98.7 ± 1.5	
OST_11.1	0.00	404	433	1.10	63.35 ± 0.87	0.0547 ± 0.0024	101.0 ± 1.4	100.1 ± 1.4	D, N
OST_12.1	0.05	312	167	0.55	63.05 ± 1.13	0.0470 ± 0.0052	101.4 ± 1.8	101.5 ± 1.7	
OST_13.1	0.00	326	235	0.74	65.68 ± 1.16	0.0447 ± 0.0026	97.4 ± 1.7	97.4 ± 1.7	
OST_14.1	0.40	303	218	0.74	67.20 ± 1.14	0.0600 ± 0.0062	95.2 ± 1.6	93.8 ± 1.5	
OST_15.1	0.22	282	164	0.60	62.80 ± 1.20	0.0448 ± 0.0054	101.8 ± 1.9	102.1 ± 1.9	
OST_16.1	0.00	117	59	0.52	70.19 ± 1.59	0.0493 ± 0.0057	91.2 ± 2.0	91.0 ± 2.1	
OST_17.1	0.76	206	134	0.67	68.66 ± 1.22	0.0563 ± 0.0079	93.2 ± 1.7	92.2 ± 1.6	
OST_18.1	0.06	377	231	0.63	64.52 ± 1.06	0.0501 ± 0.0045	99.1 ± 1.6	98.9 ± 1.6	
OST_19.1	0.00	402	371	0.95	67.53 ± 0.96	0.0474 ± 0.0024	94.8 ± 1.3	94.8 ± 1.3	
OST_19.2	1.48	166	85	0.53	67.52 ± 1.41	0.0540 ± 0.0075	94.8 ± 2.0	94.1 ± 2.0	
OST_20.1	0.00	219	116	0.54	67.07 ± 1.19	0.0452 ± 0.0030	95.4 ± 1.7	95.4 ± 1.7	
OST_21.1	0.35	353	235	0.68	66.95 ± 1.28	0.0466 ± 0.0054	95.6 ± 1.8	95.7 ± 1.8	
OST_22.1	0.00	215	151	0.72	61.99 ± 1.02	0.0526 ± 0.0036	103.2 ± 1.7	102.6 ± 1.7	
OST_23.1	0.00	267	141	0.54	65.62 ± 1.38	0.0496 ± 0.0028	97.5 ± 2.0	97.3 ± 2.1	
OST_24.1	0.08	214	128	0.62	69.48 ± 1.52	0.0491 ± 0.0062	92.1 ± 2.0	92.0 ± 2.0	
Kotatejima Islamd (KTT)									
KTT_01.1	0.00	132	102	0.79	62.57 ± 1.55	0.0491 ± 0.0043	102.2 ± 2.5	102.1 ± 2.6	N
KTT_02.1	0.39	253	165	0.67	64.91 ± 1.09	0.0541 ± 0.0054	98.6 ± 1.6	97.8 ± 1.6	N
KTT_03.1	0.00	130	87	0.69	59.81 ± 1.39	0.0455 ± 0.0039	106.9 ± 2.5	106.9 ± 2.5	N
KTT_04.1	0.00	151	98	0.67	58.01 ± 1.01	0.0457 ± 0.0037	110.2 ± 1.9	110.2 ± 1.9	N
KTT_05.1	0.00	147	105	0.73	62.96 ± 1.25	0.0455 ± 0.0040	101.6 ± 2.0	101.6 ± 2.0	N
KTT_06.1	0.00	78	53	0.70	64.27 ± 2.02	0.0454 ± 0.0055	99.5 ± 3.1	99.5 ± 3.1	N
KTT_07.1	0.34	208	107	0.53	59.89 ± 1.20	0.0414 ± 0.0054	106.7 ± 2.1	107.1 ± 2.1	N
KTT_08.1	0.00	422	441	1.07	61.90 ± 0.87	0.0505 ± 0.0023	103.3 ± 1.4	103.0 ± 1.5	N
KTT_09.1	0.00	85	55	0.67	57.01 ± 1.53	0.0489 ± 0.0045	112.1 ± 3.0	112.0 ± 3.0	N
KTT_10.1	1.71	124	79	0.65	66.42 ± 1.58	0.0355 ± 0.0081	96.3 ± 2.3	97.8 ± 2.3	N
KTT_11.1	2.38	122	92	0.78	49.88 ± 1.08	0.0332 ± 0.0077	128.0 ± 2.7	130.4 ± 2.7	N
KTT_12.1	2.51	234	146	0.64	61.31 ± 1.30	0.0520 ± 0.0065	104.3 ± 2.2	103.8 ± 2.1	N
KTT_13.1	2.10	255	142	0.57	56.05 ± 1.27	0.0376 ± 0.0066	114.0 ± 2.6	115.5 ± 2.5	N
KTT_14.1	1.69	94	49	0.54	44.72 ± 1.31	0.0675 ± 0.0136	142.5 ± 4.1	139.3 ± 3.9	N
KTT_15.1	0.00	142	103	0.75	59.09 ± 1.30	0.0582 ± 0.0045	108.2 ± 2.4	106.8 ± 2.4	D, N
KTT_16.1	0.00	440	269	0.63	61.17 ± 0.85	0.0451 ± 0.0021	104.5 ± 1.4	104.5 ± 1.4	N
KTT_17.1	0.00	705	404	0.59	54.77 ± 0.77	0.0510 ± 0.0018	116.6 ± 1.6	116.3 ± 1.6	N
KTT_18.1	1.35	241	107	0.45	55.72 ± 1.47	0.0393 ± 0.0061	114.7 ± 3.0	115.9 ± 3.0	N
Otateshima Island (OTT)									
OTT_01.1	2.05	130	80	0.63	64.10 ± 1.56	0.0343 ± 0.0092	99.8 ± 2.4	101.5 ± 2.3	
OTT_02.1	0.00	129	90	0.71	64.11 ± 1.45	0.0478 ± 0.0038	99.8 ± 2.2	99.8 ± 2.2	
OTT_03.1	4.79	545	507	0.95	67.37 ± 1.16	0.0384 ± 0.0095	95.0 ± 1.6	96.1 ± 1.6	
OTT_04.1	0.20	132	91	0.70	61.05 ± 1.33	0.0424 ± 0.0067	104.7 ± 2.3	104.9 ± 2.2	N
OTT_05.1	0.00	107	77	0.74	61.28 ± 1.38	0.0418 ± 0.0037	104.4 ± 2.3	104.4 ± 2.3	N
OTT_06.1	1.03	383	184	0.49	52.37 ± 1.14	0.0422 ± 0.0043	121.9 ± 2.6	122.9 ± 2.6	N
OTT_07.1	0.29	454	306	0.69	65.91 ± 1.00	0.0492 ± 0.0043	97.1 ± 1.5	96.9 ± 1.4	
OTT_08.1	0.73	109	98	0.92	61.60 ± 1.37	0.0373 ± 0.0084	103.8 ± 2.3	104.6 ± 2.1	N
OTT_09.1	1.30	360	364	1.04	72.57 ± 1.48	0.0636 ± 0.0063	88.2 ± 1.8	86.5 ± 1.7	D, N
OTT_10.1	0.13	140	158	1.16	62.89 ± 1.69	0.0419 ± 0.0108	101.7 ± 2.7	101.8 ± 2.4	
OTT_11.1	0.00	523	928	1.82	68.19 ± 0.90	0.0477 ± 0.0020	93.8 ± 1.2	93.8 ± 1.2	
OTT_12.1	0.72	176	168	0.98	60.60 ± 1.39	0.0440 ± 0.0089	105.5 ± 2.4	106.0 ± 2.2	N
OTT_13.1	0.00	455	667	1.50	68.34 ± 0.87	0.0545 ± 0.0019	93.6 ± 1.2	92.9 ± 1.2	D, N
OTT_13.2	0.00	160	100	0.64	62.95 ± 1.22	0.0535 ± 0.0038	101.6 ± 2.0	100.9 ± 2.0	
OTT_14.1	0.00	102	72	0.72	63.31 ± 1.25	0.0538 ± 0.0046	101.0 ± 2.0	100.3 ± 2.0	
OTT_15.1	0.00	254	153	0.62	63.78 ± 1.11	0.0504 ± 0.0033	100.3 ± 1.7	100.0 ± 1.8	
OTT_16.1	0.66	304	417	1.41	52.18 ± 0.82	0.0609 ± 0.0068	122.4 ± 1.9	120.5 ± 1.7	N
OTT_17.1	0.00	119	68	0.59	65.08 ± 1.56	0.0579 ± 0.0050	98.3 ± 2.3	97.1 ± 2.4	
OTT_18.1	0.00	73	55	0.77	62.43 ± 1.72	0.0610 ± 0.0064	102.4 ± 2.8	100.8 ± 2.9	D, N
OTT_19.1	0.00	247	182	0.76	66.06 ± 1.14	0.0532 ± 0.0028	96.8 ± 1.7	96.2 ± 1.7	
OTT_20.1	0.00	175	197	1.15	62.88 ± 1.12	0.0563 ± 0.0037	101.7 ± 1.8	100.7 ± 1.8	D, N
OTT_21.1	2.49	101	97	0.98	66.43 ± 1.91	0.0554 ± 0.0121	96.3 ± 2.7	95.4 ± 2.6	
OTT_22.1	2.05	1378	390	0.29	66.10 ± 0.73	0.0426 ± 0.0027	96.8 ± 1.1	97.4 ± 1.1	
OTT_23.1	0.00	283	340	1.23	69.43 ± 1.12	0.0551 ± 0.0026	92.2 ± 1.5	91.3 ± 1.5	D, N
OTT_24.1	0.92	207	226	1.12	68.25 ± 1.33	0.0443 ± 0.0088	93.8 ± 1.8	94.2 ± 1.7	
OTT_24.2	0.32	311	278	0.92	67.31 ± 1.29	0.0518 ± 0.0064	95.1 ± 1.8	94.6 ± 1.7	

Table 1. Continued.

Labels	$^{206}Pb_c$ (1) (%)	U (ppm)	Th (ppm)	Th/U	$^{238}U/^{206}Pb^*$ (1)	$^{207}Pb^*/^{206}Pb^*$ (1)	$^{238}U-^{206}Pb^*$ age(1) (Ma)	$^{238}U-^{206}Pb^*$ age(2) (Ma)	Remarks
OTT_25.1	1.78	113	64	0.58	66.86 ± 1.60	0.0525 ± 0.0072	95.7 ± 2.3	95.2 ± 2.2	
OTT_26.1	0.74	145	149	1.06	66.88 ± 1.74	0.0450 ± 0.0107	95.7 ± 2.5	96.0 ± 2.3	
OTT_27.1	1.51	116	75	0.67	65.81 ± 1.67	0.0307 ± 0.0097	97.2 ± 2.4	98.7 ± 2.3	
OTT_28.1	0.00	146	112	0.78	64.09 ± 1.36	0.0525 ± 0.0040	99.8 ± 2.1	99.2 ± 2.2	
OTT_28.2	0.45	263	135	0.53	66.63 ± 1.38	0.0476 ± 0.0049	96.0 ± 2.0	96.1 ± 2.0	
Irose Islet (IRS)									
IRS_01.1	0.00	134	88	0.67	64.35 ± 1.49	0.0455 ± 0.0040	99.4 ± 2.3	99.4 ± 2.3	
IRS_02.1	0.00	81	50	0.64	62.67 ± 1.63	0.0585 ± 0.0060	102.1 ± 2.6	100.7 ± 2.7	
IRS_03.1	0.36	124	79	0.66	58.67 ± 1.63	0.0436 ± 0.0076	109.0 ± 3.0	109.3 ± 2.9	N
IRS_04.1	1.98	133	78	0.60	65.99 ± 1.59	0.0519 ± 0.0089	97.0 ± 2.3	96.5 ± 2.3	
IRS_05.1	0.00	221	122	0.57	63.96 ± 1.14	0.0503 ± 0.0033	100.0 ± 1.8	99.7 ± 1.8	
IRS_06.1	0.00	157	173	1.13	61.64 ± 1.22	0.0423 ± 0.0038	103.7 ± 2.0	103.7 ± 2.0	
IRS_06.2	2.59	331	254	0.79	66.47 ± 1.25	0.0747 ± 0.0094	96.3 ± 1.8	93.0 ± 1.7	D, N
IRS_07.1	0.68	146	129	0.91	60.95 ± 1.58	0.0400 ± 0.0091	104.9 ± 2.7	105.6 ± 2.5	
IRS_08.1	0.63	135	124	0.94	63.07 ± 1.56	0.0407 ± 0.0087	101.4 ± 2.5	102.0 ± 2.3	
IRS_09.1	0.00	108	75	0.72	61.35 ± 1.50	0.0498 ± 0.0046	104.2 ± 2.5	104.0 ± 2.6	
IRS_10.1	0.37	298	125	0.43	63.58 ± 1.18	0.0451 ± 0.0042	100.6 ± 1.8	101.0 ± 1.8	
IRS_11.1	0.00	169	138	0.84	63.18 ± 1.29	0.0526 ± 0.0040	101.2 ± 2.0	100.7 ± 2.1	
IRS_12.1	0.00	112	100	0.92	65.17 ± 1.60	0.0569 ± 0.0045	98.2 ± 2.4	97.1 ± 2.4	
IRS_13.1	0.05	99	69	0.72	61.57 ± 1.75	0.0424 ± 0.0095	103.9 ± 2.9	103.9 ± 2.7	
IRS_13.2	0.00	132	80	0.62	62.49 ± 1.46	0.0498 ± 0.0041	102.3 ± 2.4	102.1 ± 2.4	
IRS_14.1	0.00	231	230	1.02	63.56 ± 1.42	0.0517 ± 0.0037	100.6 ± 2.2	100.2 ± 2.3	
IRS_15.1	0.00	418	296	0.73	66.11 ± 1.00	0.0452 ± 0.0022	96.8 ± 1.5	96.8 ± 1.5	
IRS_16.1	0.00	628	397	0.65	61.72 ± 0.91	0.0518 ± 0.0021	103.6 ± 1.5	103.1 ± 1.5	
IRS_17.1	0.00	135	95	0.73	66.52 ± 1.58	0.0499 ± 0.0042	96.2 ± 2.3	95.9 ± 2.3	
IRS_18.1	0.00	257	252	1.01	60.68 ± 1.20	0.0454 ± 0.0029	105.4 ± 2.1	105.4 ± 2.1	
IRS_19.1	0.00	86	56	0.67	60.63 ± 1.63	0.0421 ± 0.0047	105.5 ± 2.8	105.5 ± 2.8	
IRS_20.1	0.00	168	139	0.85	62.60 ± 1.41	0.0489 ± 0.0032	102.2 ± 2.3	102.1 ± 2.3	
IRS_20.2	1.06	654	243	0.38	64.88 ± 0.94	0.0424 ± 0.0032	98.6 ± 1.4	99.3 ± 1.4	
IRS_21.1	0.00	67	46	0.71	61.08 ± 1.66	0.0504 ± 0.0050	104.7 ± 2.8	104.4 ± 2.9	
IRS_22.1	1.15	127	90	0.73	61.47 ± 1.62	0.0436 ± 0.0084	104.0 ± 2.7	104.6 ± 2.7	
IRS_22.2	4.98	721	522	0.74	65.79 ± 1.00	0.0562 ± 0.0053	97.2 ± 1.5	96.3 ± 1.4	
IRS_23.1	0.00	332	362	1.12	67.60 ± 0.98	0.0487 ± 0.0024	94.7 ± 1.4	94.6 ± 1.4	
IRS_24.1	0.00	216	123	0.58	61.20 ± 0.97	0.0529 ± 0.0032	104.5 ± 1.6	103.9 ± 1.7	
IRS_25.1	0.00	309	241	0.80	64.14 ± 1.08	0.0482 ± 0.0027	99.7 ± 1.7	99.7 ± 1.7	
IRS_26.1	0.00	102	70	0.71	63.30 ± 1.54	0.0479 ± 0.0044	101.1 ± 2.4	101.1 ± 2.4	
IRS_27.1	0.00	295	339	1.18	67.88 ± 0.98	0.0474 ± 0.0029	94.3 ± 1.4	94.3 ± 1.4	
IRS_27.2	1.88	1745	1401	0.82	65.18 ± 0.75	0.0514 ± 0.0026	98.2 ± 1.1	97.7 ± 1.1	
IRS_28.1	0.02	151	107	0.73	64.64 ± 1.62	0.0405 ± 0.0072	99.0 ± 2.5	99.0 ± 2.3	
IRS_29.1	2.30	390	223	0.59	63.75 ± 1.17	0.0432 ± 0.0054	100.3 ± 1.8	101.0 ± 1.8	
IRS_30.1	0.00	115	119	1.06	64.66 ± 1.63	0.0444 ± 0.0039	98.9 ± 2.5	98.9 ± 2.5	
IRS_31.1	0.85	126	79	0.65	65.28 ± 1.58	0.0440 ± 0.0084	98.0 ± 2.3	98.5 ± 2.3	
IRS_32.1	1.14	245	117	0.49	59.36 ± 1.22	0.0398 ± 0.0067	107.7 ± 2.2	108.8 ± 2.1	N
IRS_33.1	1.79	92	61	0.68	65.12 ± 1.90	0.0444 ± 0.0100	98.2 ± 2.8	98.7 ± 2.8	
IRS_34.1	0.34	194	117	0.62	67.33 ± 1.41	0.0489 ± 0.0064	95.0 ± 2.0	94.9 ± 1.9	
IRS_35.1	1.13	157	99	0.65	58.65 ± 1.34	0.0357 ± 0.0068	109.0 ± 2.5	110.2 ± 2.4	N
IRS_36.1	0.21	421	249	0.61	58.87 ± 0.91	0.0447 ± 0.0035	108.6 ± 1.7	108.8 ± 1.6	N
Enoshima Island (ENS)									
ENS_01.1	0.02	442	291	0.68	65.41 ± 1.37	0.0471 ± 0.0057	97.8 ± 2.0	97.8 ± 2.0	
ENS_02.1	0.00	614	609	1.02	63.65 ± 1.03	0.0460 ± 0.0024	100.5 ± 1.6	100.5 ± 1.6	
ENS_03.1	0.00	298	241	0.83	61.72 ± 1.24	0.0478 ± 0.0033	103.6 ± 2.1	103.6 ± 2.1	
ENS_04.1	0.00	599	583	1.00	64.31 ± 1.00	0.0475 ± 0.0024	99.5 ± 1.5	99.5 ± 1.5	
ENS_05.1	0.30	232	164	0.73	62.16 ± 1.48	0.0529 ± 0.0077	102.9 ± 2.4	102.3 ± 2.3	
ENS_06.1	0.00	823	1001	1.25	65.50 ± 0.91	0.0484 ± 0.0020	97.7 ± 1.4	97.6 ± 1.4	
ENS_07.1	0.00	674	1091	1.66	62.64 ± 1.08	0.0484 ± 0.0022	102.1 ± 1.7	102.0 ± 1.8	
ENS_08.1	0.00	1027	1215	1.21	65.72 ± 0.82	0.0489 ± 0.0018	97.3 ± 1.2	97.2 ± 1.2	
ENS_09.1	0.00	1514	2569	1.74	61.86 ± 0.74	0.0504 ± 0.0015	103.4 ± 1.2	103.1 ± 1.2	
ENS_10.1	0.83	140	64	0.47	64.79 ± 1.68	0.0426 ± 0.0080	98.7 ± 2.5	99.4 ± 2.5	
ENS_11.1	1.21	249	191	0.79	62.01 ± 1.41	0.0387 ± 0.0077	103.1 ± 2.3	104.3 ± 2.2	
ENS_12.1	0.07	510	448	0.90	63.34 ± 1.24	0.0446 ± 0.0061	101.0 ± 2.0	101.0 ± 1.8	
ENS_13.1	0.04	289	165	0.59	60.43 ± 1.22	0.0499 ± 0.0060	105.8 ± 2.1	105.6 ± 2.1	
ENS_14.1	0.71	127	116	0.94	58.75 ± 1.83	0.0467 ± 0.0124	108.8 ± 3.4	109.0 ± 3.1	N
ENS_15.1	0.00	202	110	0.56	64.16 ± 1.55	0.0391 ± 0.0035	99.7 ± 2.4	99.7 ± 2.4	D, N
ENS_16.1	0.41	663	606	0.94	61.23 ± 0.91	0.0459 ± 0.0052	104.4 ± 1.5	104.7 ± 1.5	
ENS_17.1	0.00	794	860	1.11	64.99 ± 0.75	0.0485 ± 0.0020	98.4 ± 1.1	98.4 ± 1.2	
ENS_18.1	0.54	185	90	0.50	65.39 ± 1.75	0.0424 ± 0.0069	97.8 ± 2.6	98.4 ± 2.5	
ENS_19.1	0.00	176	93	0.54	64.56 ± 1.68	0.0435 ± 0.0040	99.1 ± 2.6	99.1 ± 2.6	
ENS_20.1	0.00	607	486	0.82	62.68 ± 0.88	0.0481 ± 0.0021	102.0 ± 1.4	102.0 ± 1.4	
ENS_21.1	0.00	840	1163	1.42	59.55 ± 0.79	0.0470 ± 0.0019	107.4 ± 1.4	107.4 ± 1.4	N
ENS_22.1	0.69	87	61	0.72	63.38 ± 2.39	0.0453 ± 0.0140	100.9 ± 3.8	101.3 ± 3.6	
ENS_23.1	0.64	179	122	0.70	62.63 ± 1.51	0.0431 ± 0.0084	102.1 ± 2.4	102.7 ± 2.4	
ENS_24.1	0.00	753	798	1.09	65.95 ± 0.97	0.0502 ± 0.0022	97.0 ± 1.4	96.7 ± 1.4	
ENS_25.1	0.00	129	57	0.45	66.67 ± 1.83	0.0545 ± 0.0056	96.0 ± 2.6	95.2 ± 2.7	

Table 1. Continued.

Labels	$^{206}Pb_c$ [(1)] (%)	U (ppm)	Th (ppm)	Th/U	$^{238}U/^{206}Pb^{*(1)}$	$^{207}Pb^{*}/^{206}Pb^{*(1)}$	$^{238}U–^{206}Pb^{*}$ age[(1)] (Ma)	$^{238}U–^{206}Pb^{*}$ age[(2)] (Ma)	Remarks
ENS_26.1	0.00	191	86	0.46	62.52 ± 1.39	0.0547 ± 0.0043	102.3 ± 2.2	101.4 ± 2.3	
ENS_27.1	0.31	125	56	0.45	63.40 ± 1.75	0.0435 ± 0.0087	100.9 ± 2.8	101.2 ± 2.6	
ENS_28.1	0.00	401	295	0.76	63.60 ± 1.26	0.0492 ± 0.0033	100.6 ± 2.0	100.4 ± 2.0	
ENS_29.1	0.66	469	365	0.80	64.21 ± 1.29	0.0453 ± 0.0059	99.6 ± 2.0	100.0 ± 1.9	
ENS_30.1	0.00	120	72	0.62	60.69 ± 1.72	0.0408 ± 0.0048	105.3 ± 3.0	105.3 ± 3.0	
ENS_31.1	0.00	105	64	0.63	65.11 ± 2.28	0.0453 ± 0.0063	98.3 ± 3.4	98.3 ± 3.4	
ENS_32.1	0.00	116	85	0.75	60.81 ± 1.68	0.0488 ± 0.0059	105.1 ± 2.9	105.1 ± 3.0	
ENS_33.1	2.84	496	394	0.81	63.77 ± 1.16	0.0394 ± 0.0070	100.3 ± 1.8	101.4 ± 1.7	
ENS_34.1	0.28	460	347	0.77	59.35 ± 1.07	0.0430 ± 0.0047	107.7 ± 1.9	108.0 ± 1.9	N
Hirukojima Island (HRK)									
HRK_01.1	0.26	116	76	0.68	62.01 ± 1.50	0.0478 ± 0.0077	103.1 ± 2.5	103.2 ± 2.4	
HRK_02.1	0.00	86	60	0.72	63.79 ± 1.79	0.0516 ± 0.0059	100.3 ± 2.8	99.8 ± 2.9	
HRK_03.1	0.00	79	49	0.64	63.04 ± 2.02	0.0495 ± 0.0053	101.5 ± 3.2	101.3 ± 3.3	
HRK_04.1	0.00	443	409	0.95	65.27 ± 1.13	0.0506 ± 0.0025	98.0 ± 1.7	97.7 ± 1.7	
HRK_05.1	0.00	85	51	0.62	62.50 ± 1.97	0.0424 ± 0.0047	102.3 ± 3.2	102.3 ± 3.2	
HRK_06.1	2.06	141	129	0.94	63.78 ± 1.74	0.0330 ± 0.0103	100.3 ± 2.7	102.2 ± 2.6	
HRK_07.1	1.75	164	101	0.63	64.06 ± 1.67	0.0430 ± 0.0075	99.9 ± 2.6	100.5 ± 2.5	
HRK_08.1	0.22	119	64	0.55	61.76 ± 1.52	0.0506 ± 0.0074	103.5 ± 2.5	103.2 ± 2.5	
HRK_09.1	0.00	110	85	0.79	59.79 ± 1.57	0.0566 ± 0.0052	106.9 ± 2.8	105.8 ± 2.8	
HRK_10.1	1.83	124	84	0.70	67.34 ± 1.81	0.0328 ± 0.0097	95.0 ± 2.5	96.8 ± 2.4	
HRK_11.1	0.16	174	88	0.52	61.73 ± 1.39	0.0520 ± 0.0059	103.6 ± 2.3	103.1 ± 2.3	
HRK_12.1	0.00	107	67	0.64	62.59 ± 1.58	0.0538 ± 0.0053	102.2 ± 2.6	101.4 ± 2.6	
HRK_13.1	0.00	125	74	0.61	58.85 ± 1.43	0.0461 ± 0.0036	108.6 ± 2.6	108.6 ± 2.6	
HRK_14.1	0.88	254	155	0.62	63.02 ± 1.19	0.0436 ± 0.0055	101.5 ± 1.9	102.1 ± 1.9	
HRK_15.1	1.80	75	46	0.63	65.48 ± 2.14	0.0315 ± 0.0118	97.7 ± 3.2	99.5 ± 3.0	
HRK_16.1	1.11	155	104	0.69	62.23 ± 1.37	0.0418 ± 0.0070	102.8 ± 2.2	103.6 ± 2.2	
HRK_17.1	1.04	147	98	0.68	60.79 ± 1.42	0.0373 ± 0.0076	105.2 ± 2.4	106.3 ± 2.3	
HRK_18.1	0.20	92	55	0.61	63.41 ± 1.86	0.0529 ± 0.0092	100.9 ± 2.9	100.3 ± 2.9	
HRK_19.1	3.23	168	110	0.67	65.00 ± 1.50	0.0388 ± 0.0084	98.4 ± 2.3	99.6 ± 2.2	
HRK_20.1	0.00	131	100	0.79	62.74 ± 1.32	0.0548 ± 0.0046	101.9 ± 2.1	101.1 ± 2.2	
HRK_20.2	0.62	165	106	0.66	59.37 ± 1.32	0.0433 ± 0.0063	107.7 ± 2.4	108.3 ± 2.3	
HRK_21.1	0.00	94	90	0.98	62.79 ± 1.79	0.0477 ± 0.0043	101.9 ± 2.9	101.9 ± 2.9	
HRK_22.1	0.38	91	53	0.60	63.77 ± 1.97	0.0634 ± 0.0097	100.3 ± 3.1	98.4 ± 3.0	
HRK_23.1	1.04	137	74	0.56	62.57 ± 1.64	0.0481 ± 0.0071	102.2 ± 2.7	102.2 ± 2.6	
HRK_24.1	1.09	69	50	0.75	60.47 ± 1.98	0.0338 ± 0.0100	105.7 ± 3.4	106.9 ± 3.3	
HRK_25.1	0.09	127	117	0.95	61.84 ± 1.71	0.0442 ± 0.0110	103.4 ± 2.8	103.5 ± 2.6	
HRK_26.1	0.61	300	118	0.40	57.36 ± 0.99	0.0433 ± 0.0039	111.4 ± 1.9	112.1 ± 1.9	N
HRK_27.1	1.80	166	113	0.70	65.29 ± 1.44	0.0339 ± 0.0082	98.0 ± 2.1	99.7 ± 2.1	

Errors are 1-sigma; Pb_c and Pb^* indicate the common and radiogenic portions, respectively.
Remarks; D: discordant, N: not used for weighted mean age calculation
(1) Common Pb corrected by assuming $^{206}Pb/^{238}U–^{208}Pb/^{232}Th$ age-concordance
(2) Common Pb corrected by assuming $^{206}Pb/^{238}U–^{207}Pb/^{235}U$ age-concordance

1.2 Ma (n = 8; MSWD = 1.48; when OST, KTT, OTT, IRS and HRK were analyzed) and 32.8 ± 2.2 Ma (n = 5; MSWD = 3.28; when ENS was analyzed). MSWD is acronym of mean square weighted deviation, which is calculated from square root of χ^2 value.

Sample Descriptions and Age Results of Zircon

Table 1 lists zircon data in terms of the fraction of common ^{206}Pb, U, and Th concentrations, Th/U, $^{238}U/^{206}Pb^*$ and $^{207}Pb^*/^{206}Pb^*$ ratios, and radiometric $^{238}U/^{206}Pb^*$ ages of the samples. All errors reported therein are at the 1σ level. All zircons in the samples show rhythmic oscillatory and/or sector zoning in CL images (Fig. 4), which is commonly observed in igneous zircons (e.g. Corfu *et al.*, 2003). Errors of weighted mean zircon U–Pb ages are reported at a 95% confidence interval (95% conf.). Concordia and age distribution diagrams are shown in Figs. 5 and 6, respectively. The obtained weighted mean ages and sample localities are summarized in Table 2.

All rock samples are stored in the National Museum of Nature and Science. The registration number of each sample can be found from the rock specimen number in the collection database of the National Museum of Nature and Science (http://db.kahaku.go.jp/webmuseum_en/).

OST: Oseto granodiorite

The sample was collected from the northwestern end of the Nishisonogi Peninsula (lat: N32°59′17.29″, long: E129°38′13.95″). This is a medium grained biotite-hornblende granite. The major minerals of this rock are alkali feldspar, plagioclase, quartz,

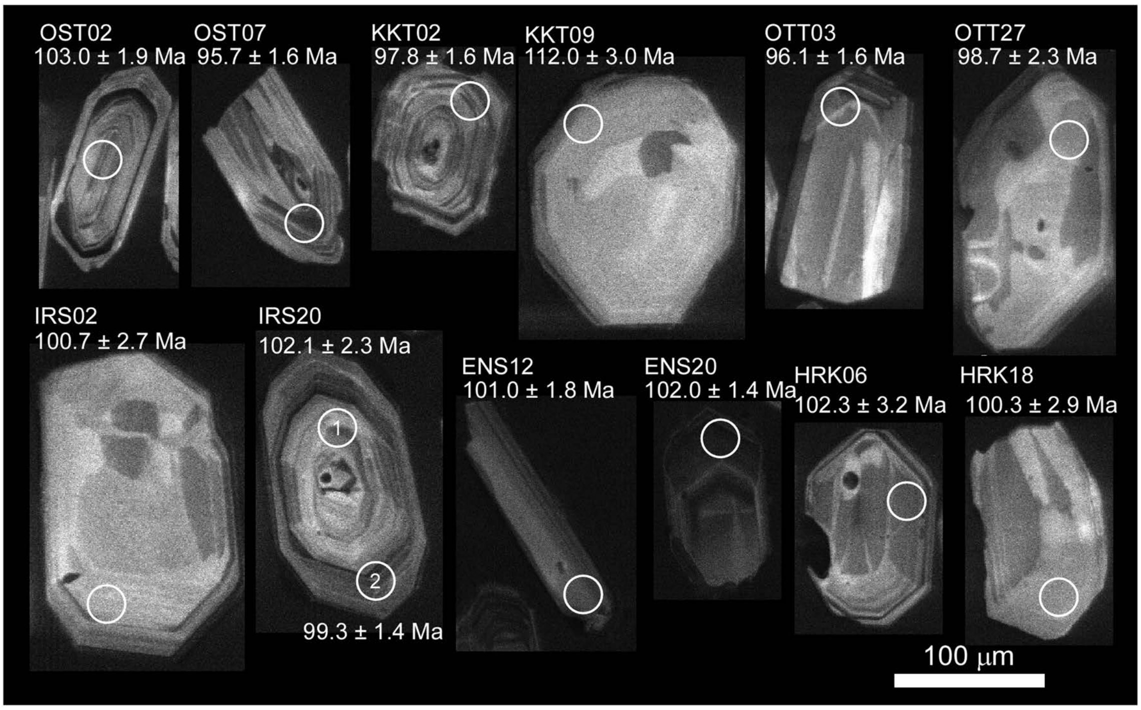

Fig. 4. Cathodoluminescence images of analyzed section of typical zircon grains from the samples. Circles in the images indicate points analyzed by LA-ICP-MS and are approximately 25 μm in diameter.

amphibole, and biotite. Plagioclase occurs as euhedral to subhedral crystals and exhibits indistinct albite twin and oscillatory zoning. Undulatory extinction is observed in quartz. Zircon and opaque mineral are common accessory minerals. The registration number is 137823.

Most zircon grains were prismatic and 60 to 260 μm in length with an elongation ratio ranging from 1.6 to 3.8. 26 spots from 24 grains were analyzed and 25 data were concordant. However, the weighted mean age of the sample was not effective because the age data were widely spread between 91 and 104 Ma. The rough approximated weighted mean age was 97 ± 2 Ma (MSWD = 4.18).

KTT: Kotatejima Island

The sample was collected from Kotatejima Island, which is situated between Enoshima Island and the Nishisonogi Peninsula (lat: N33°0′17.52″, long: E129°27′3.77″). This is a medium grained biotite-hornblende granodiorite. The major minerals of this rock are plagioclase, quartz, alkali feldspar, biotite and amphibole. Plagioclase occurs as euhedral to subhedral crystals and exhibits indistinct albite twin and oscillatory zoning. Undulatory extinction is observed in quartz. Zircon and opaque mineral are common accessory minerals. The registration number is 137825.

Most zircon grains were prismatic and 120 to 230 μm in length with a short elongation ratio ranging from 1.2 to 2.5. 19 spots from 19 grains were analyzed and 18 data were concordant. However, an effective weighted mean age could not be obtained from the sample because the age data were spread in a wide range from 92 to 140 Ma.

OTT: Otateshima Island

The sample was collected from Otateshima Island, which is the largest island between Enoshima Island and the Nishisonogi Peninsula (lat: N33°1′17.01″, long: E129°26′3.73″). This is a medium grained biotite granodiorite. The major minerals of this rock are plagioclase, quartz, alkali feldspar, and biotite. Biotite is totally altered into chlorite. Plagioclase occurs as euhedral to subhedral crystal and exhibits indistinct albite twin and oscillatory zoning. Undulatory extinction is observed in quartz. Zircon and opaque mineral are common accessory minerals. The registration number is 137827.

Most zircon grains were prismatic and 100 to 190 μm in length with an elongation ratio from 2.0 to 4.0. 31 spots from 28 grains were analyzed and 26 data were concordant. After 6 old data were excluded, the weighted mean age of 20 data was

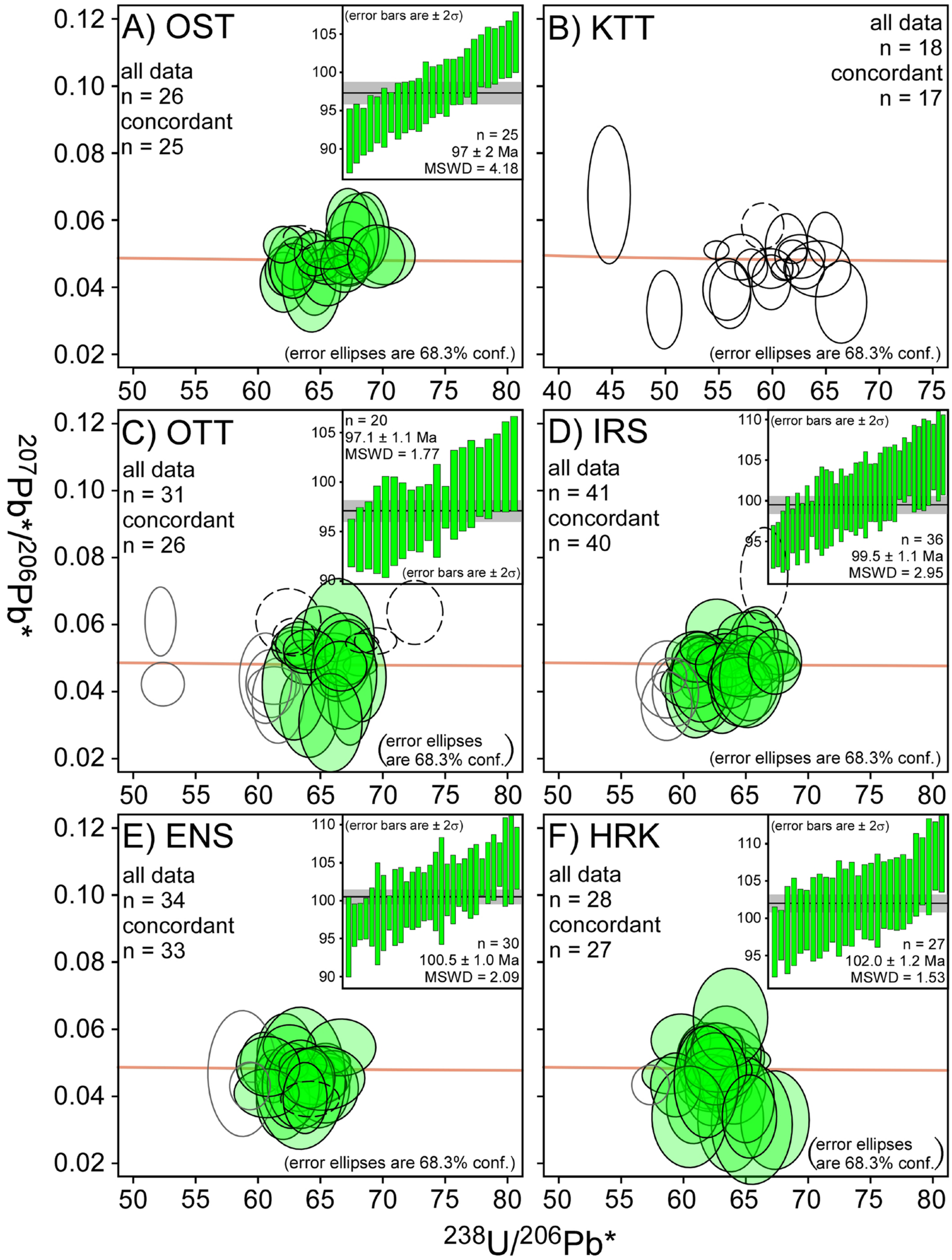

Fig. 5. Tera–Wasserberg U–Pb concordia diagrams and age distribution plots of zircons from the samples. Solid ellipses: concordant data; Broken ellipses: discordant data; Filled ellipses: data used for age calculation.

97.1 ± 1.1 Ma (MSWD = 1.77).

IRS: Irose Islet

The sample was collected from Irose Islet, which is flattened small islet situated between Enoshima Island and the Nishisonogi Peninsula (lat: N33°1′58.85″, long: E130°50′51.0″). This is a medium grained hornblende-biotite granodiorite. The major minerals of this rock are quartz, plagioclase, alkali feldspar, biotite and amphibole. Plagioclase occurs as euhedral to subhedral crystal and exhibits indistinct albite twin and oscillatory zoning. Undulatory extinction is observed in quartz. Zircon and opaque mineral are common accessory minerals. The registration number is 137828.

Most zircon grains were prismatic and 150 to 270 μm in length with an elongation ratio ranging from 1.7 to 3.9. 41 spots from 36 grains were analyzed and 40 data were concordant. After 4 old data were excluded, the weighted mean age of all concordant data was 99.5 ± 1.1 Ma (MSWD = 2.95).

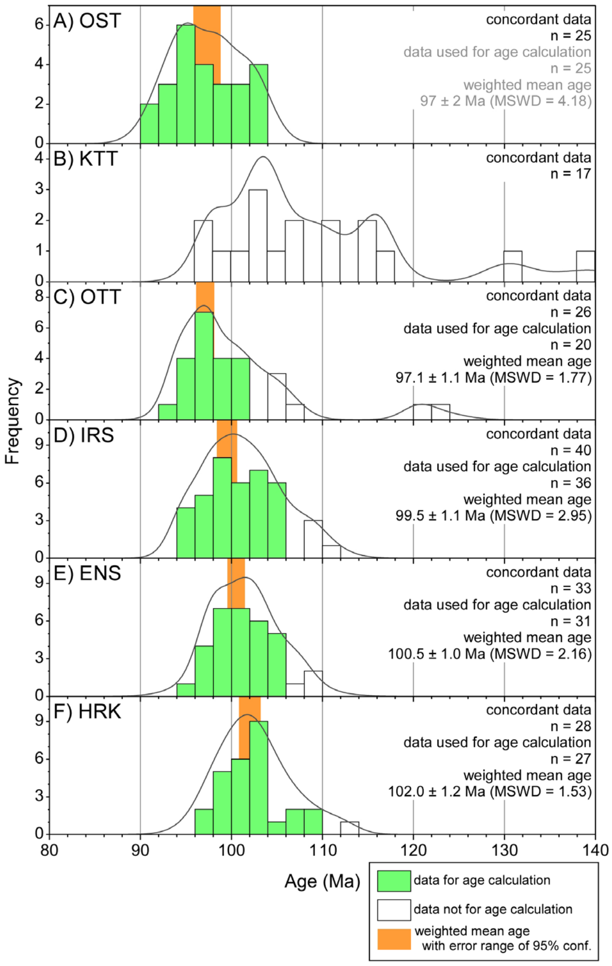

Fig. 6. Probability density diagrams and histogram of zircon ages in the samples.

ENS: granitic intrusion in Enoshima Island

The sample was collected from a granitic dyke intruding into andesite which is correlated to the Early Cretaceous Kanmon Group (lat: N33°0′17.52″, long: E129°26′3.49″). This is a fine grained hornblende-biotite granodiorite. The major minerals of this rock are plagioclase, quartz, alkali feldspar, amphibole and biotite. Plagioclase occurs as euhedral to subhedral crystal and exhibits indistinct albite twin and oscillatory zoning. Undulatory extinction is observed in quartz. Zircon and opaque mineral are common accessory minerals. The registration number is 137830.

Most zircon grains were prismatic and 70 to 220 μm in length with an elongation ratio ranging from 1.2 to 6.0. 34 spots from 34 grains were analyzed and all data were concordant. After 3 old data were excluded, the weighted mean age of 31 data was 100.5 ± 1.0 Ma (MSWD = 2.16).

HRK: granitic mass of Hirukojima Island

The sample was collected from Hirukojima Island, a small island adjacent to Enoshima Island, consisting of granodiorite mass (lat: N33°0′17.38″, long: E129°27′3.44″). This is a fine grained biotite-hornblende granodiorite. The major minerals of this rock are plagioclase, quartz, alkali feldspar, amphibole and biotite. Plagioclase occurs as euhedral to subhedral crystal and exhibits indistinct albite twin and oscillatory zoning. Undulatory extinction is observed in quartz. Zircon and opaque mineral are common accessory minerals. The registration number is 137829.

Most zircon grains were prismatic and 130 to 240 μm in length with a short elongation ratio ranging from 1.5 to 4.4. 28 spots from 27 grains were analyzed and all data were concordant. After an old datum was

Table 2. Summary of the localities and weighted mean ages of the studied samples.

sample name	reg. No.[1]	rock type	locality	n of data			Age	
				All	Conc.	Calc.		MSWD
OST	137823	biotite-hornblende granite	N32°59′17.29″E129°38′13.95″	26	25	25	(97 ± 2)	4.18
KTT	137825	biotite-hornblende granodiorite	N33°00′17.52″E129°27′03.77″	18	17	—	—	
OTT	137827	biotite granodiorite	N33°01′17.01″E129°26′03.73″	31	26	20	97.1 ± 1.1	1.77
IRS	137828	hornblende-biotite granodiorite	N33°01′58.85″E129°25′10.37”	41	40	36	99.5 ± 1.1	2.95
ENS	137830	hornblende-biotite granodiorite	N32°59′59.35″E129°21′07.83″	34	33	30	100.5 ± 1.0	2.16
HRK	137829	biotite-hornblende granodiorite	N32°59′56.53″E129°20′55.50″	28	28	27	102.0 ± 1.2	1.53

Age errors are 95% conf.; Conc.: concordant, Calc.: used for age calculation.

1) The redistration number of rock specimen in the collection database of the National Museum of Nature and Science (http://db.kahaku.go.jp/webmuseum_en/).

excluded, the weighted mean age of 27 concordant data was 102.0 ± 1.2 Ma (MSWD = 1.53).

Discussion

Formation age of the Nishisonogi granites

Although effective ages of the samples OST and KTT were not obtained, zircon U–Pb ages were obtained from the OTT, IRS, ENS and HRK samples to be 97.1 ± 1.1 Ma, 99.5 ± 1.1 Ma, 100.5 ± 1.0 Ma and 102.0 ± 1.2 Ma, respectively. Considering the probability density curve of these age data, the weighted mean ages overlap the modes of the probability density curves (Fig. 6 C–F). However, the weighted mean age of OST is aways older than the mode (Fig. 6 A). This suggests that inherited zircons whose ages were older and close to those of magmatic zircons were contained in the OST sample and that the OST formation age is ~95 Ma as indicated by the mode of the probability density curve. The formation ages of the Nishisonogi granites range from 102 to 95 Ma, and the ages become older toward the west, i.e. continental side.

The age of KTT can be inferred as 99–97 Ma based on the zircon ages of neighboring OTT and IRS. However, the zircon age spectrum of the sample KTT is without a definite peak, and most of the individual ages of zircons show older ages than the inferred age (Fig. 6B). These zircon grains can be regarded as inherited grains distinguished from zircon grains formed at the granitoid formation age. It suggests that the source magma of KTT had already been saturated in zirconium and was not able to dissolve additional zircon grains (for the theoretical rationale, see Boehnke *et al.*, 2013; Watson and Harrison, 1983). Additionally, it is thought that the magma was saturated in zirconium at too low content to crystalize new zircon grains when the magma solidified. As a similar example has been found in the Nabaenohana tonalite in the Kurosegawa belt (Aoki *et al.*, 2015), granitoids lacking synchro-plutonism zircon grains are not unusual.

Attribution of the Nishisonogi granites

The Nagasaki metamorphic rocks in the Nishisonogi Peninsula show an N–S trend (Noda and Muta, 1957; Uchida and Muta, 1957) as is the case with the Yobikonoseto TL strike. The Cretaceous Nishisonogi granites (Tachibana, 1962) lie on the continental side of this TL. The positional relationship among these high -P/T type metamorphics, TL and granitoids is similar to the one among the Sanbagawa belt, MTL and Ryoke belt (e.g. Miyashiro, 1965), suggesting that the Nishisonogi granites represent the western extension of the Ryoke belt. This hypothesis is reinforced by the newly obtained fact that the NMC in the Nishisonogi Peninsula is attributed to the Sanbagawa belt (e.g., Kochi *et al.*, 2011). Zircon U–Pb ages of the Nishisonogi granites (102–95 Ma) are similar to granitoids in the Yanai area (105–95 Ma; Skrzypek *et al.*, 2016) at the western end of the Ryoke and Sanyo belts. On these lines of chronological evidence, at a glance it might seem safe to conclude that the Nishisonogi granites are the western extension of the Ryoke and Sanyo belts.

However, while the ages of granitoids in the Ryoke and Sanyo belts become younger toward the continental side (e.g. Iizumi and Imaoka, 2009; Iida *et al.*, 2015), those of the Nishisonogi granites become older. As the reason for this difference in age trend remains unclear, it is still premature to conclude that the Nishisonogi granites are the western extension of the Ryoke and Sanyo belts.

K–Ar and zircon U–Pb ages of Cretaceous granitoids in Nagasaki

The zircon U–Pb ages of the Nishisonogi granites obtained in this study are 102–95 Ma while previously determined K–Ar ages were 93–89 Ma (Hattori and Shibata, 1982. Kawano and Ueda, 1966). Nagata *et al.* (2020) similarly reported a zircon U–Pb age of 118.0 ± 0.8 Ma for granite in Kabashima from which biotite and muscovite K–Ar ages had been previously reported as 93–77 Ma (Hattori and Shibata, 1982; Nishimura, 1998). K–Ar ages have been regarded to represent the cooling age after plutonism because of their lower closure temperature than other radiometric ages (e.g. Osanai *et al.*, 2006). However, the presence of surficial exposed granite of ＜1 Ma in age (e.g. Ito *et al.*, 2013) provides evidence that the cooling rate of granitoids can be much faster than previously thought. Moreover, because the Nishisonogi granites are shallow intrusions (Isomi *et al.*, 1971), it is likely that they cooled faster than ordinary granitoids. Thus, it is impractical to regard K–Ar ages as cooling ages. Then, the question remains as to how much lower the K–Ar ages are than zircon ages indicate.

One possibility is rejuvenation by Ar dissipation from dated minerals through weathering. An extreme case is a K–Ar age of "biotite" reported from granitoid in the Mogi area. Although the "biotite K–Ar age" was reported as 54.1 ± 7.1 Ma for this granitoid (Igi *et al.*, 1976: recalculated), there was actually no biotite preserved in the rock. Instead, only biotite pseudomorphs which were totally composed of chlorite were present with a zircon U–Pb age of 117.1 ± 0.4 Ma (Tsutsumi and Horie, 2019). In this case, the "biotite K–Ar age" did not provide any information on the cooling age of the granitoid body.

Another possibility is rejuvenation through thermal effects of unexposed younger granitoids, although currently no evidence is available supporting this hypothesis. Re-examination of K–Ar ages of Cretaceous granitoids in Nagasaki Prefecture would provide a clue to resolve this issue.

Acknowledgment

The author thanks Ms. Y. Kusaba of the National Museum of Nature and Science for her help in SEM analysis. This work is conducted as a part of the project "Interpreting geological meanings of granitoids in southwest Japan" of the National Museum of Nature and Science.

References

Aoki, K., Isozaki, Y., Yamamoto, A., Sakata, S. and Hirata, T. (2015) Mid-Paleozoic arc granitoids in SW Japan with Neoproterozoic xenocrysts from South China: New zircon U–Pb ages by LA-ICP-MS. *Journal of Asian Earth Sciences*, **97**: 125–135.

Black, L. P., Kamo, S. L., Allen, C. M., Davis, D. W., Aleinikoff, J. N., Valley, J. W., Mundil, R., Campbell, I. H., Korsch, R. J., Williams, I. S. and Foudoulis, C. (2004). Improved $^{206}Pb/^{238}U$ microprobe geochronology by the monitoring of a trace-element-related matrix effect; SHRIMP, ID-TIMS, ELA-ICP-MS and oxygen isotope documentation for a series of zircon standards. *Chemical Geology*, **205**: 115–140.

Boehnke, P., Watson, E. B., Trail, D., Harrison, T. M. and Schmitt, A. K. (2013) Zircon saturation re-revisited. *Chemical Geology*, **351**: 324–334.

Corfu, F., Hanchar, J. M., Hoskin, P. W. O. and Kinny, P. (2003) An atlas of zircon textures. In: Hanchar, J. M. and Hoskin, P. W. O. (Eds.), *Zircon: Reviews in Mineralogy and Geochemistry 53*, Mineralogical Society of America, Washington D.C., USA, pp. 469–500.

Hattori, H., Inoue, E. and Matsui, K. (1993) *Geology of the Konoura district*, *quadrangle series*, *1 : 50000*. Geological Survey of Japan, AIST, Tsukuba, Japan (in Japanese with English abstract).

Hattori, H. and Shibata, K. (1982) Radiometric dating of Pre-Neogene granitic and metamorphic rocks in northwest Kyushu, Japan -with emphasis on geotectonic of the Nishisonogi zone. *Bulletin of the Geological Survey of Japan*, **33**: 57–84.

Igi, S., Shibata, K. and Hattori, H. (1976) On the rock of 400 Ma in the Nagasaki Metamorphic Rocks. *Tooko Kiban*, **3**: 45–46 (in Japanese)*.

Iida, K., Iwamori, H., Orihashi Y., Park, T., Jwa, Y.-J., Kwon, S.-T., Danhara, T. and Iwano, H. (2015). Tectonic reconstruction of batholith formation based on the spatiotemporal distribution of Cretaceous–Paleogene granitic rocks in southwestern Japan. *Island Arc*, **24**: 205–220.

Iizumi, S. and Imaoka, T. (2009) Radiometric ages. In: Geological Society of Japan (Ed.), *Monograph on Geology of Japan*, *Vol. 6*, *Chugoku*, Asakura Publishing, Tokyo, Japan, pp. 324–327 (in Japanese)*.

Isomi, H., Matsui, K., Katada, M., Kawada, K., Nagahama, H., Hattori, H. and Kamada, Y. (1971) The geology of the Tsushima and Goto Islands and surrounding sea areas. *Preprint papers for the symposium on the geological problems in Kyushu and its sea areas*: 27–37 (In Japanese).*

Ito, H., Yamada, R., Tamura, A., Arai, S., Horie, K. and Hokada, T. (2013) Earth's youngest exposed granite and its tectonic implications: The 10–0.8 Ma Kurobegawa Granite. *Scientific Reports*, **3**: 1306.

Iwano, H., Orihashi, Y., Hirata, T., Ogasawara, M., Danhara, T., Horie, K., Hasebe, N., Sueoka, S., Tamura, A., Hayasaka, Y., Katsube, A., Ito, H., Tani, K., Kimura, J., Chang, Q., Kouchi, Y., Haruta, Y. and Yamamoto, K. (2013) An inter-laboratory evaluation of OD-3 zircon for use as a secondary U–Pb dating standard. *Island Arc*, **22**: 382–394.

Karakida, Y., Yamomoto, H., Miyachi, S., Oshima, T. and Inoue, T. (1969) Characteristics and geological situations of metamorphic rocks in Kyushu. *Memoirs of the Geological Society of Japan*, **4**: 3–21 (in Japanese with English abstract).

Katada, M., Nagahama, H., Matsui, K., Hattori, H. and Isomi, H. (1972) *Geology of the Hizen-Enoshima district*, *quadrangle series*, *1 : 50000*. Geological Survey of Japan, AIST, Tsukuba, Japan (in Japanese with English abstract).

Katsura, T. (1992) Submarine geology in the vicinity of Tsushima-Goto Retto region. *Report of Hydrographic Researches*, **28**: 55–138 (in Japanese with English abstract).

Kawano, M. and Ueda, Y. (1966) K-Ar dating on the igneous rocks in Japan (V): Granitic rocks in southwestern Japan. *Journal of Mineralogy*, *Petrology and Economic Geology*, **56**: 191–211 (in Japanese with English abstract).

Kimura, M., Hiroshima, T., Onodera, K. and Shimizu, A. (1975) *Submarine Geological Map Around Koshikijima*

Island, *1 : 200000*. Geological Survey of Japan, AIST, Tsukuba, Japan (in Japanese with English legends).

Kouchi, Y., Orihashi, Y., Obara, H., Miyata, K., Simojo, M., Otoh, S., Aoyama, M., Akahori, Y. and Yanai, S. (2011) Discovery of Shimanto high-P/T metamorphic rocks from the western margin of Kyushu, Japan. *Journal of Geography (Chigaku Zasshi)*, **120**: 30–39 (in Japanese with English abstract).

Miyashiro, A. (1965) Metamorphic belts and metamorphic rocks. Iwanami Shoten Publishers, Tokyo, Japan, 458p. (in Japanese)*.

Miyazaki, K., Ikeda, T., Arima, K., Fukuyama, M., Maki, K., Yui, T.-F. and Grove, M. (2013). Pressure–temperature structure of a mylonitized metamorphic pile, and the role of advection of the lower crust, Nagasaki Metamorphic Complex, Kyushu, Japan. *Lithos*, **162–163**: 14–26.

Nagata, M., Kouchi, Y. and Otoh, S. (2020) Early Cretaceous U–Pb dates of zircons from the Kabashima granite in the Nomo Peninsula, Nagasaki Prefecture, SW Japan. *Journal of the Geological Society of Japan*, **126**: 333–339 (in Japanese with English abstract).

Nishimura, Y. (1998). Geotectonic subdivision and areal extent of the Sangun belt, Inner Zone of Southwest Japan. *Journal of metamorphic Geology* **16**: 129–140.

Nishimura, Y., Hirota, Y., Shiosaki, D., Nakahara, N. and Itaya, T. (2004). The Nagasaki metamorphic rocks and their geotectonics in Mogi area, Nagasaki Prefecture, Southwest Japan—Juxtaposition of the Suo belt with the Sanbagawa belt—. *Journal of the Geological Society of Japan*, **110**: 372–383 (in Japanese with English abstract).

Noda, M. and Muta, K. (1957) The structure of the Nishisonogi Peninsula, Nagasaki Prefecture. *Reports on earth science*, *Department of General Education*, *Kyushu University*, **4**: 17–21 (in Japanese with English abstract).

Osanai, Y., Owada, M., Kamei, A., Hamamoto, T., Kagami, H., Toyoshima, T., Nakano, N. and Nam, T. N. (2006) The Higo metamorphic complex in Kyushu, Japan as the fragment of Permo–Triassic metamorphic complexes in East Asia. *Gondwana Research*, **9**: 152–166.

Skrzypek, E., Kawakami, T., Hirajima, T., Sakata, S. Hirata, T. and Ikeda, T. (2016). Revisiting the high temperature metamorphic field gradient of the Ryoke Belt (SW Japan): New constraints from the Iwakuni-Yanai area. *Lithos*, **260**: 9–27.

Stacey, J. S. and Kramers, J. D. (1975) Approximation of terrestrial lead isotope evolution by a two–stage model. *Earth and Planetary Science Letters*, **26**: 207–221.

Tachibana, K. (1962) On the pre-Tertiary Enoshima Formation, Ainoshima thermally metamorphosed rocks and the Cretaceous Nishisonogi granitic rocks exposed on the sea between the Goto Islands and the Nishisonogi Peninsula: In special reference to the granitic rocks of Nagasaki Prefecture. Bulletin of Faculty of Liberal Arts, Nagasaki University. *Natural Science*, **3**, 24–43 (in Japanese with English abstract).

Tsutsumi, Y. and Horie, K. (2019) Zircon U–Pb age of the granitic tectonic block between the Suo Metamorphic Belt and Nagasaki Metamorphic Complex, Nagasaki Peninsula, southwest Japan. *Bulletin of the National Museum of Nature and Science*, *Series C*, **45**: 7–12.

Tsutsumi, Y., Horie, K., Sano, T., Miyawaki, R., Momma, K., Matsubara, S., Shigeoka, M. and Yokoyama, K. (2012) LA-ICP-MS and SHRIMP ages of zircons in chevkinite and monazite tuffs from the Boso Peninsula, Central Japan. *Bulletin of the National Museum of Nature and Science*, *Series C*, **38**: 15–32.

Tsutsumi, Y., Yokoyma, K., Terada, K. and Sano, Y. (2003): SHRIMP U–Pb dating of detrital zircons in metamorphic rocks from the northern Kyushu, western Japan. *Journal of Mineralogical and Petrological Sciences*, **98**: 181–193.

Tunheng, A and Hirata, T. (2004) Development of signal smoothing device for precise elemental analysis using laser ablation-ICP-mass spectrometry. *Journal of Analytical Atomic Spectrometry*, **7**: 932–934.

Uchida, Y. and Muta, K. (1957) The Talc Deposits in Northern Kyusyu (I): Distribution and Types of the Talc Deposits. *Journal of the Geological Society of Japan*, **63**, 589–597 (in Japanese with English abstract).

Vermeesch, P. (2018) IsoplotR: A free and open toolbox for geochronology. *Geoscience Frontiers*, **9**: 1479–1493.

von Richthofen, F. (1903). Geomorphologische Studien aus Ostasien (IV. Über Gebirgskettungen in Ostasien, mit Ausschluss von Japan. V. Gebirgskettungen im japanischen Bogen). Sitzungsber der Königlichen, Preussischen Akademie der Wissenschaften, Stück XL (physikalisch-mathematischen), 52p. (in Germany).

Watson, E. B. and Harrison, T. M. (1983) Zircon saturation revisited: temperature and composition effects in a variety of crustal magma types. *Earth and Planetary Science Letters*, **64**: 295–304.

Williams, I. S. (1998) U–Th–Pb geochronology by ion microprobe. In: McKibben, M. A., Shanks, W. C. P. and Ridley, W. I. (Eds.), *Applications of Microanalytical Techniques to Understanding Mineralizing Processes. Reviews in Economic Geology 7*, Society of Economic Geologists, Littleton, CO. USA, pp. 1–35.

* English translation from the original written in Japanese.